Journal of Holography Applications in Physics
Volume 7, Issue 2, Spring 2027, xx–xx
©Available online at http://jhap.du.ac.ir
DOI: 10.22128/jhap.2026.3246.1190
Online ISSN: 2783–3518

Regular article

Late-Time Cosmology in $f(Q,B)$ Gravity: Insights from Holographic and Barrow Holographic Dark Energy Models

Amit Samaddar[1] · S. Surendra Singh[2]

[1] Department of Mathematics, National Institute of Technology Manipur, Imphal-795004, India;
Corresponding Author E-mail: samaddaramit4@gmail.com

[2] Department of Mathematics, National Institute of Technology Manipur, Imphal-795004, India;
E-mail: ssuren.mu@gmail.com

Received: February 8, 2026; **Accepted:** June 13, 2026

Abstract. We investigate holographic dark energy and Barrow holographic dark energy models within the framework of modified gravity based on non-metricity and boundary contributions. The cosmological evolution of the Universe is examined using a phenomenological expansion history constrained by a joint analysis of cosmic chronometer, DESI DR2 baryon acoustic oscillation, and Pantheon+ supernova datasets. The observational results are consistent with the standard cosmological scenario and show mild improvement in addressing the Hubble tension. The reconstructed dark energy equation of state remains in the quintessence regime throughout the cosmic evolution. The analysis of energy conditions indicates that the null and dominant energy conditions are satisfied, while the strong energy condition is violated, supporting the observed late-time accelerated expansion of the Universe. The model predicts a transition from decelerated to accelerated expansion at a redshift consistent with recent observations and yields an age of the Universe compatible with current estimates. A comparative study shows that the Barrow holographic dark energy model exhibits a smoother and more stable late-time evolution than the standard holographic dark energy model. These results suggest that entropy corrections associated with Barrow holography can enhance the dynamical properties of dark energy in modified gravity and provide a viable description of the late-time cosmic acceleration.

Keywords: $f(Q,B)$ Gravity; Holographic and Barrow Holographic Dark Energy; Observational Cosmology; Dark Energy Dynamics.

Contents

1 Introduction

Understanding the origin, evolution and large-scale behavior of the Universe remains a central goal of modern cosmology. Over the past decades, a wealth of observational data, like Type Ia supernovae distances, cosmic microwave background (CMB) fluctuations and baryon acoustic oscillations (BAO), has established that the Universe is currently undergoing accelerated expansion [1,2]. The standard Lambda Cold Dark Matter (ΛCDM) model attributes this acceleration to dark energy, a mysterious component constituting roughly 70% of the cosmic energy budget, while dark matter and baryons account for about 25% and 5%, respectively. Despite its observational successes, the nature of dark energy remains unknown. In ΛCDM, it is described by a cosmological constant Λ with an equation of state $\omega = \frac{p}{\rho} = -1$, implying a constant energy density. However, the model suffers from theoretical issues, such as the fine-tuning and coincidence problems, motivating the development of alternative and dynamical dark energy models [3,4].

The success of the standard cosmological model has not diminished the motivation to seek extensions of Einstein's General Relativity (GR), as several of its fundamental issues remain unresolved. Although GR provides an exceptionally accurate description of gravitational phenomena on solar and galactic scales, it faces challenges when applied to the earliest and largest phases of cosmic evolution. Problems such as the initial singularity, the unexplained cause of the present cosmic acceleration, and the mysterious nature of dark matter and dark energy suggest that GR may be incomplete at cosmological scales. These open questions have led to the development of various modified gravity theories that aim to account for the observed acceleration of the universe without introducing unknown matter components. Among the most studied are curvature-based $f(R)$ gravity [5,6], torsion-based $f(T)$ gravity [7,8], and matter-coupled frameworks such as $f(R,T)$ and $f(Q,L_m)$ gravities [9,10], each providing alternative geometric pathways to describe cosmic dynamics.

An important step forward in this context comes from the geometric trinity of gravity, which allows gravitation to be represented in terms of curvature, torsion, or nonmetricity. Within this framework, the symmetric teleparallel approach describes gravity entirely through the nonmetricity scalar Q, assuming both curvature and torsion vanish [11]. The simplest extension, known as $f(Q)$ gravity, can successfully explain late-time cosmic acceleration and early-Universe inflation. However, it can be further generalized by including the boundary term B, related to Q via the relation $R = -Q + B$. This leads to the $f(Q,B)$ gravity framework [12], which unifies the geometric features of both $f(Q)$ and $f(R)$ theories, offering a more comprehensive formulation to describe the universe's evolution. Recent research has shown that $f(Q,B)$ models provide stable cosmological solutions, reproduce dark energy behavior, and remain consistent with current observational constraints [13–15]. Building upon these developments, the present work adopts $f(Q,B)$ gravity as the theoretical foundation to study the cosmological behavior of dark energy models.

Another promising perspective on explaining the Universe's late-time acceleration is offered by the holographic principle, which connects quantum gravity and cosmology by relating the Universe's energy content to its boundary geometry. Originally proposed by 't Hooft and Susskind [16,17], this principle states that all the physical information contained within a volume can be represented through degrees of freedom defined on its boundary surface. When incorporated into cosmology, it imposes a restriction on the quantum vacuum energy, ensuring that the total energy enclosed within a region of size L does not exceed the mass of a black hole of the same radius. This condition leads to the formulation of the Holographic Dark Energy (HDE) model, where the dark energy density scales inversely with the square of the IR cutoff length, $\rho_D \propto L^{-2}$ [18,19]. The selection of this IR cutoff critically shapes the resulting cosmic evolution—whether based on the Hubble horizon, event horizon, or Granda–Oliveros (G–O) cutoff, each choice yields distinct dynamical behaviors. In particular, the G–O cutoff, which depends on both H and $\dot{H}$, introduces a dynamic component to dark energy that successfully addresses the causality issues associated with event-horizon models and remains consistent with observational constraints [20,21]. Overall, HDE models provide a compelling phenomenological link between cosmic acceleration and the underlying effects of quantum gravity.

Recent developments highlight that the conventional HDE model is based on the classical Bekenstein–Hawking entropy–area relation, which may not hold in regimes where quantum gravitational effects become significant. To overcome this limitation, Barrow proposed a modified entropy–area relation incorporating a fractal deformation parameter that accounts for potential quantum-gravitational corrections to the horizon geometry [22]. This modification gives rise to the Barrow Holographic Dark Energy (BHDE) model, wherein the dark energy density exhibits an additional dependence on the deformation parameter Δ. The BHDE model extends the standard HDE scenario, recovering it as a special case when $\Delta = 0$. A nonzero Δ represents deviations from a smooth spacetime geometry, effectively encoding possible quantum fluctuations of the horizon. This generalized formulation enhances the theoretical flexibility of holographic dark energy, enabling a broader range of cosmological behaviors and successfully describing late-time cosmic acceleration in agreement with observational constraints [23–25]. A number of studies have indicated that the BHDE model naturally accounts for the cosmic transition from matter domination to dark energy domination, producing stable late-time solutions that align well with observational evidence. In particular, employing the Hubble horizon as the infrared cutoff offers a simple and physically meaningful description of the Universe's evolution, achieved without introducing extra free parameters. This simplicity and consistency make the BHDE framework especially attractive within modified gravity scenarios, where the interaction between holographic energy density and geometric modifications can have a profound impact on the dynamics of cosmic expansion [26–29].

In light of these developments, this work explores the HDE and BHDE models within the framework of $f(Q, B)$ gravity. This approach enables a detailed study of how the combined effects of nonmetricity and boundary terms influence the dynamics of holographic dark energy and its extensions. Using an observationally constrained Hubble function, based on the CC46, DESI DR2 BAO, and Pantheon+ datasets, we perform a comprehensive analysis of the cosmic expansion history, energy conditions, and diagnostic parameters. The aim is to determine whether $f(Q, B)$ gravity can provide a consistent geometric explanation for dark energy and the Universe's accelerated expansion, while also highlighting the distinct cosmological features of the HDE and BHDE models.

The remainder of this paper is organized as follows. In section 2, we present the fundamental field equations of the $f(Q, B)$ gravity framework and introduce a non-linear functional form for the model. Section 3 is dedicated to the cosmological reconstruction using an observationally motivated Hubble parameter $H(z)$ with constraints from the CC46, DESI DR2 BAO, and Pantheon+ datasets. In section 4, we study the HDE and BHDE models within the $f(Q, B)$ framework and analyze their evolution under the chosen Hubble function. The behavior of essential cosmological diagnostics including the deceleration parameter, the $Om(z)$ diagnostic and the age of the Universe is discussed in sections 5, 6 and 7 respectively. Finally, section 8 summarizes the main results, highlights their broader implications, and suggests possible directions for future research.

2 Field equations and model formulation in $f(Q, B)$ gravity

A distinct geometrical formulation of gravitation can be established by employing nonmetricity as the fundamental geometric quantity, in contrast to curvature, which underlies General Relativity (GR). Within the general metric–affine approach, the affine connection can be decomposed into three independent components: curvature, torsion, and nonmetricity. The torsion tensor, which captures the antisymmetric aspect of the connection, is expressed as

$$T^{\eta}{}_{\epsilon\zeta} = \Gamma^{\eta}{}_{\epsilon\zeta} - \Gamma^{\eta}{}_{\zeta\epsilon}. \tag{2.1}$$

In contrast to torsion and curvature, the nonmetricity tensor characterizes the extent to which the metric tensor fails to be preserved when it is parallelly transported along a curve. This tensor is mathematically formulated as

$$Q_{\eta\epsilon\zeta} \equiv \nabla_{\eta} g_{\epsilon\zeta} = \partial_{\eta} g_{\epsilon\zeta} - \Gamma^{\mu}_{\eta\epsilon} g_{\mu\zeta} - \Gamma^{\mu}_{\eta\zeta} g_{\epsilon\mu}. \tag{2.2}$$

Within the framework of symmetric teleparallel geometry, both curvature and torsion are constrained to vanish, i.e. $R^{\mu}{}_{\epsilon\zeta} = 0$ and $T^{\mu}{}_{\epsilon\zeta} = 0$, so that nonmetricity remains as the only geometric feature describing the connection. These constraints are naturally realized in the coincident gauge, wherein all components of the affine connection are set to zero [30],

$$\Gamma^{\eta}{}_{\epsilon\zeta} = 0. \tag{2.3}$$

With the adoption of this gauge, covariant differentiation simplifies to an ordinary derivative, so that the nonmetricity tensor assumes the following form:

$$Q_{\eta\epsilon\zeta} = \nabla_{\eta} g_{\epsilon\zeta}. \tag{2.4}$$

Using this definition, two trace-like quantities of the nonmetricity tensor are defined by

$$Q_{\eta} = Q_{\eta}{}^{\epsilon}\epsilon, \qquad \widetilde{Q}\eta = Q^{\epsilon}{}_{\eta\epsilon}. \tag{2.5}$$

In constructing the dynamical sector of the theory, a superpotential tensor $P^{\eta}{}_{\epsilon\zeta}$ is introduced, given by

$$P^{\eta}{}_{\epsilon\zeta} = \frac{1}{4}\left[-Q^{\eta}{}_{\epsilon\zeta} + 2Q_{(\epsilon}{}^{\eta}{}_{\zeta)} - Q^{\eta} g_{\epsilon\zeta} + \bar{Q}^{\eta} g_{\epsilon\zeta} - \delta^{\eta}_{(\epsilon} Q_{\zeta)}\right], \tag{2.6}$$

and is characterized by symmetry with respect to its lower indices ϵ and ζ.

In analogy with General Relativity, where the Ricci scalar encapsulates curvature effects, the nonmetricity scalar is formulated by contracting the nonmetricity tensor with the superpotential as

$$Q = -Q_{\eta\epsilon\zeta} P^{\eta\epsilon\zeta}. \tag{2.7}$$

The relation between the Ricci scalar of the Levi-Civita connection and the nonmetricity scalar is established through a boundary term:

$$R = -Q + B, \tag{2.8}$$

where

$$B = \frac{2}{\sqrt{-g}}\,\partial_{\epsilon}\left(\sqrt{-g}\,Q^{\epsilon}\right), \tag{2.9}$$

represents the corresponding surface contribution. Consequently, the Einstein–Hilbert action can be equivalently expressed in terms of the nonmetricity scalar Q and the boundary contribution B. Although the term B does not affect the field equations in conventional General Relativity, it becomes significant in the extended framework of $f(Q,B)$ gravity. In these modified theories, the explicit dependence of the action on Q and B introduces additional dynamical degrees of freedom, giving rise to observable departures from GR and enabling a broader range of gravitational and cosmological phenomena.

When the matter Lagrangian density is incorporated, the total action of the theory becomes

$$S = \int d^4x\sqrt{-g}\left[\frac{1}{2\kappa}f(Q,B) + \mathcal{L}_m\right]. \tag{2.10}$$

When the action is varied with respect to the metric tensor, one obtains the dynamical equations of the theory, encapsulating its gravitational properties. These equations are given by:

$$\begin{aligned}\kappa T_{\epsilon\zeta} &= -\frac{f}{2}g_{\epsilon\zeta} + \frac{2}{\sqrt{-g}}\partial_\eta\left(\sqrt{-g}f_Q P^\eta{}_{\epsilon\zeta}\right) + \left[P_{\epsilon\alpha\beta}Q_\zeta{}^{\alpha\beta} - 2P_{\alpha\beta\zeta}Q^{\alpha\beta}{}_\epsilon\right]f_Q \\ &\quad + \left(\frac{B}{2}g_{\epsilon\zeta} - \mathring{\nabla}_\epsilon\mathring{\nabla}_\zeta + g_{\epsilon\zeta}\mathring{\nabla}^\alpha\mathring{\nabla}_\alpha - 2P^\eta{}_{\epsilon\zeta}\partial_\eta\right)f_B.\end{aligned} \tag{2.11}$$

A covariant reformulation of these equations reveals the explicit geometric and physical structure of the theory. Here, the Einstein tensor of GR is modified by additional terms arising from nonmetricity and the associated boundary term.

$$\begin{aligned}\kappa T_{\epsilon\zeta} &= -\frac{f}{2}g_{\epsilon\zeta} + \frac{2}{\sqrt{-g}}P^\eta{}_{\epsilon\zeta}\nabla_\eta(f_Q - f_B) + \left[\mathring{G}_{\epsilon\zeta} + \frac{Q}{2}g_{\epsilon\zeta}\right]f_Q \\ &\quad + \left(\frac{B}{2}g_{\epsilon\zeta} - \mathring{\nabla}_\epsilon\mathring{\nabla}_\zeta + g_{\epsilon\zeta}\mathring{\nabla}^\alpha\mathring{\nabla}_\alpha\right)f_B.\end{aligned} \tag{2.12}$$

By reorganizing the extra geometrical contributions into an effective energy–momentum tensor, one can cast the equations into a form resembling Einstein's equations, resulting in a compact and physically meaningful representation:

$$T^{\text{eff}}_{\epsilon\zeta} = T_{\epsilon\zeta} + \frac{1}{\kappa}\left[\frac{f}{2}g_{\epsilon\zeta} - 2P^\eta{}_{\epsilon\zeta}\nabla_\eta(f_Q - f_B) - \frac{1}{2}Qf_Q g_{\epsilon\zeta} - \left(\frac{B}{2}g_{\epsilon\zeta} - \mathring{\nabla}_\epsilon\mathring{\nabla}_\zeta + g_{\epsilon\zeta}\mathring{\nabla}^\alpha\mathring{\nabla}_\alpha\right)f_B\right], \tag{2.13}$$

Within this formulation, all departures from standard General Relativity are incorporated into the effective energy–momentum tensor $T^{\text{eff}}_{\epsilon\zeta}$, which captures the additional geometric influences arising from nonmetricity and the boundary term. From a cosmological standpoint, this framework introduces novel dynamical degrees of freedom capable of reproducing dark energy–like effects or driving late-time cosmic acceleration. The mutual interaction between Q and B enriches the model's phenomenology, providing a flexible approach to studying cosmic evolution beyond the scope of the ΛCDM paradigm.

In $f(Q,B)$ gravity, the gravitational field equations can be expressed in a manner analogous to the Einstein equations, highlighting the correspondence between the modified and standard formulations.

$$\mathring{G}_{\epsilon\zeta} = \frac{\kappa}{f_Q}T^{\text{eff}}_{\epsilon\zeta}, \tag{2.14}$$

Here, $\mathring{G}_{\epsilon\zeta}$ represents the Einstein tensor computed using the Levi-Civita connection.

For studying the cosmological dynamics of the theory, we consider a flat, homogeneous, and isotropic spacetime background, reflecting the observed large-scale properties of the Universe. This is represented by the Friedmann-Lemaître-Robertson-Walker (FLRW) metric in Cartesian form:

$$ds^2 = -dt^2 + a^2(t)(dx^2 + dy^2 + dz^2), \tag{2.15}$$

The function $a(t)$ represents the cosmic scale factor, tracking the expansion of space over time. The expansion rate is captured by the Hubble parameter, $H(t) = \dot{a}(t)/a(t)$, where the overdot denotes a derivative with respect to time. This cosmological framework underpins the study of both the evolutionary dynamics and observational predictions within $f(Q, B)$ gravity.

In $f(Q, B)$ cosmology, the modifications to the field equations introduce geometric contributions that extend beyond the standard matter content. These additional terms can be interpreted as a geometrically induced dark energy, whose energy–momentum tensor is defined as:

$$T^{(\mathrm{DE})}_{\epsilon\zeta} = \frac{1}{f_Q}\left[\frac{f}{2}g_{\epsilon\zeta} - 2P^{\eta}{}_{\epsilon\zeta}\nabla_\eta(f_Q - f_B) - \frac{1}{2}Qf_Q g_{\epsilon\zeta} - \left(\frac{B}{2}g_{\epsilon\zeta} - \mathring{\nabla}_\epsilon\mathring{\nabla}_\zeta + g_{\epsilon\zeta}\mathring{\nabla}^\alpha\mathring{\nabla}_\alpha\right)f_B\right], \tag{2.16}$$

When this formalism is applied to a spatially flat FLRW background, the primary geometric scalars simplify to well-known relations:

$$Q = -6H^2, \quad B = 6(3H^2 + \dot{H}), \quad \mathring{R} = 6(2H^2 + \dot{H}), \tag{2.17}$$

To facilitate computations, we adopt the coincident gauge, setting the affine connection to zero, $\Gamma^{\eta}_{;\epsilon\zeta} = 0$. This choice removes inertial effects and reduces covariant derivatives to standard partial derivatives. When combined with the FLRW background, the modified field equations of $f(Q, B)$ gravity simplify to generalized Friedmann equations, which govern the Universe's expansion in this theory:

$$\kappa\rho = \frac{f}{2} + 6H^2 f_Q - (9H^2 + 3\dot{H})f_B + 3H\dot{f}_B, \tag{2.18}$$

$$\kappa p = -\frac{f}{2} - (6H^2 + 2\dot{H})f_Q - 2H\dot{f}_Q + (9H^2 + 3\dot{H})f_B - \ddot{f}_B. \tag{2.19}$$

The symbols ρ and p denote the usual cosmic energy density and pressure, respectively. The functions $f_Q = \partial f/\partial Q$ and $f_B = \partial f/\partial B$, together with their time derivatives, introduce additional geometric effects that modify the gravitational dynamics relative to GR. These effects act as a repulsive force, generating the observed accelerated expansion without the need for exotic matter. In this way, $f(Q, B)$ gravity provides a natural, purely geometric explanation for the Universe's late-time acceleration.

We now consider a specific form of the gravitational Lagrangian in the framework of $f(Q, B)$ gravity, defined as

$$f(Q, B) = \alpha Q^n + \beta B^m, \tag{2.20}$$

where α and β are coupling constants, while m and n represent the nonlinearity indices associated with the nonmetricity scalar Q and the boundary term B, respectively. The motivation for adopting this form arises from its mathematical simplicity and physical richness. The power-law structure provides a minimal yet efficient generalization of the linear case that corresponds to GR. When $m = n = 1$, the function reduces to $f(Q, B) = \alpha Q + \beta B$, which, using the identity $R = -Q + B$, recovers the Einstein–Hilbert action for a suitable choice of constants, thereby ensuring that GR is contained as a limiting case of the theory. The power-law dependence on Q and B allows us to explore deviations from the GR regime by introducing nonlinear corrections that can influence cosmological dynamics, particularly the late-time acceleration of the Universe. Such functional forms have been widely studied in other modified gravity contexts—most notably in $f(R)$, $f(T)$, $f(Q)$ and $f(Q,C)$ theories—where the ansatz $f(Q)=\alpha Q^m$, $f(R)=\alpha R^m$, $f(T)=\alpha T^m$ and $f(Q,C)=\alpha Q^n+\beta C$ successfully reproduces various cosmological behaviors, including quintessence-like and phantom-like evolutions [13–15,31–36]. Following this analogy, the inclusion of a boundary term B^n in addition to Q^m in $f(Q,B)$ gravity provides a natural generalization that captures both the pure nonmetricity contribution and the geometric boundary effects. This combination not only enriches the dynamics but also helps investigate the interplay between the two geometric scalars, which can yield effective dark energy behavior without invoking an explicit cosmological constant. Hence, this particular functional form is well motivated theoretically, consistent with known physical limits, and versatile enough to model the accelerating Universe within the symmetric teleparallel geometry.

3 Constraining the model through cosmological observations

In order to analyze the expansion dynamics in the $f(Q,B)$ framework, we employ a phenomenological description of the Hubble function given by [37]

$$H(z)=H_0\sqrt{\Omega_{m0}(1+z)^3+(1-\Omega_{m0})\left[1+\varepsilon\ln(1+z)\right]}. \tag{3.1}$$

This parameter ε encapsulates deviations from the usual cosmological scenario. This model preserves standard matter dynamics, introducing instead a slowly evolving dark-energy term whose departure from ΛCDM strengthens logarithmically with redshift. Deviations from a constant vacuum energy are a natural consequence in certain modified gravity frameworks, where geometric contributions to the cosmic budget vary gently over time. This is precisely the case in $f(Q,B)$ theories, driven by nonmetricity–boundary interactions. Notably, the model possesses a well-defined limit that restores the standard cosmology. Setting $\varepsilon=0$ causes equation (3.1) to become $H(z)=H_0\sqrt{\Omega_{m0}(1+z)^3+(1-\Omega_{m0})}$, thus exactly reproducing the flat ΛCDM expansion history as derived from GR. For a nonzero ϵ, the expansion rate diverges from ΛCDM mainly at low redshifts. The logarithmic correction evolves slowly, allowing the model to capture subtle late-time deviations while preserving the successful early-Universe dynamics. Physical consistency requires that the effective dark-energy sector does not become negative within the observational domain of redshift. Consequently, only small negative values of ε are permitted, whereas positive ε guarantees positivity for all $z\geq 0$. Accordingly, this setup is well positioned to explore slight but potentially measurable differences from a pure cosmological constant, facilitating straightforward tests against existing observations. Thus, the parameters $(H_0,\Omega_{m0},\varepsilon)$ are tested against high-precision observations, including the 46-point $H(z)$ data, DESI DR2 BAO measurements and the Pantheon+ supernova compilation, yielding strong bounds on deviations from the ΛCDM expansion predicted by $f(Q,B)$ gravity.

3.1 Parameter estimation technique

The objective of this section is to utilize the most recent observational datasets to constrain the allowable ranges of the free parameters in the model. To achieve this, we employ the Markov Chain Monte Carlo (MCMC) technique within a Bayesian statistical framework to efficiently explore the parameter space. The analysis is carried out using the Python package `emcee` [38], a well-established tool for sampling high-dimensional distributions and obtaining posterior probability distributions of cosmological parameters. In this framework, the likelihood function is assumed to follow a Gaussian form,

$$\mathcal{L} \propto \exp\left(-\frac{\chi^2}{2}\right). \tag{3.2}$$

In this formulation, χ^2 quantifies the difference between the predicted theoretical values and the observed measurements. The total chi-squared value, accounting for all the observational datasets considered in the analysis, is defined as

$$\chi^2_{\rm tot} = \chi^2_{\rm CC} + \chi^2_{\rm BAO} + \chi^2_{\rm Pantheon+}. \tag{3.3}$$

For this model, the parameters $(H_0, \Omega_{m0}, \varepsilon)$ are sampled uniformly within the prior limits

$$50 < H_0 < 100, \quad 0 < \Omega_{m0} < 1, \quad -1 < \varepsilon < 1. \tag{3.4}$$

These bounds are inspired by current cosmological observations but are intentionally kept wide to prevent any bias toward specific theoretical expectations. The MCMC sampling begins with random parameter values drawn from these priors and is performed using a substantial number of walkers and iterations. Convergence and statistical reliability are verified through diagnostics such as the autocorrelation time. By jointly analyzing the Cosmic Chronometer (CC) Hubble dataset, the DESI DR2 BAO measurements, and the Pantheon+ Type Ia Supernova sample, we derive combined constraints that tightly restrict the cosmological parameters and evaluate the consistency of the $f(Q, B)$ framework with the observed late-time expansion of the Universe. The resulting posterior distributions provide both the best-fit estimates and corresponding credible intervals for each parameter, thereby illuminating the role of geometric modifications in shaping cosmic evolution.

3.2 CC data and statistical procedure

Our first observational constraint arises from the cosmic chronometer (CC) method, which provides direct measurements of the Hubble parameter $H(z)$ at different redshifts. In this analysis, we employ a dataset comprising 46 independent measurements of $H(z)$, obtained from the differential age evolution of passively evolving galaxies [39–41]. The CC approach is particularly valuable because it is model-independent, relying solely on the differential aging of galaxies rather than assumptions about the cosmological background or the integrated luminosity distance. The core relation underlying this technique is expressed as

$$H(z) = -\frac{1}{1+z}\frac{dz}{dt}, \tag{3.5}$$

which directly connects the expansion rate to the observed age variation of galaxies across redshift intervals.

Each observational point in the dataset is denoted as $H_{\rm obs}(z_i)$ with its corresponding uncertainty σ_i, for $i = 1, 2, \ldots, 46$. The theoretical model prediction $H_{\rm th}(z_i; H_0, \Omega_{m0}, \varepsilon)$, derived from equation (3.1), is compared with the observations through a standard chi-squared minimization:

$$\chi^2_{\rm CC}(H_0, \Omega_{m0}, \varepsilon) = \sum_{i=1}^{46} \frac{[H_{\rm obs}(z_i) - H_{\rm th}(z_i; H_0, \Omega_{m0}, \varepsilon)]^2}{\sigma_i^2}. \tag{3.6}$$

This procedure provides direct constraints on the expansion rate parameters and serves as the foundation for the joint likelihood analysis when combined with BAO and Supernova datasets.

3.3 Incorporation of DESI DR2 BAO Data

To enhance the robustness of our cosmological constraints, we incorporate the most recent Baryon Acoustic Oscillation (BAO) measurements from the Dark Energy Spectroscopic Instrument (DESI) Data Release 2 (DR2). This dataset offers unprecedented precision in BAO distance estimations, obtained through galaxy and quasar clustering analyses across a broad redshift interval. The DESI DR2 sample includes over 14 million tracers collected during the first three years of survey operations [42]. Baryon Acoustic Oscillations arise from sound waves that propagated through the photon–baryon plasma in the early Universe, leaving a distinct signature in the present-day matter distribution. This characteristic scale functions as a standard cosmic ruler, allowing us to infer distance measures like the comoving angular diameter distance $D_M(z)$ and the Hubble distance $D_H(z)$ at various redshifts. In our framework, the theoretical values of these quantities are evaluated from the model-dependent Hubble rate $H(z)$ using the standard cosmological expressions:

$$D_M(z) = c\int_0^z \frac{dz'}{H(z')}, \tag{3.7}$$

$$D_H(z) = \frac{c}{H(z)}. \tag{3.8}$$

The statistical comparison between the model and the DESI DR2 BAO data is performed using a chi-squared estimator, assuming Gaussian-distributed errors for all measurements. The likelihood function is expressed as

$$\chi^2_{BAO} = \sum_i \frac{\left[D_i^{obs} - D_i^{th}(H_0, \Omega_{m0}, \delta)\right]^2}{\sigma_i^2}, \tag{3.9}$$

where D_i^{obs} denotes the observed BAO distance indicators (such as D_M/r_d and D_H/r_d) measured at redshift z_i, D_i^{th} represents the corresponding theoretical predictions derived from our model's $H(z)$, and σ_i is the observational uncertainty.

This approach enables the DESI DR2 BAO data to serve as a powerful probe of the cosmic expansion history, providing stringent constraints on the parameters of the $f(Q, B)$ model and offering a robust comparison to standard cosmological frameworks such as ΛCDM.

3.4 Constraints from the Pantheon+ Type Ia Supernova dataset

To strengthen the observational foundation of our study, we incorporate the Pantheon+ Type Ia supernova (SNe Ia) compilation — the most comprehensive and consistently processed collection of SNe Ia data available to date. The sample contains $1,701$ high-quality light curves from $1,550$ spectroscopically confirmed supernovae, spanning a redshift range of $z \approx 0.001$ to 2.26 [43,44]. With its improved calibration techniques and expanded low-redshift coverage, the Pantheon+ dataset delivers highly precise distance measurements, thereby tightening constraints on the cosmic expansion history.

The principal observable in supernova cosmology is the distance modulus, which relates the apparent and absolute magnitudes of SNeIa through

$$\mu_{th}(z) = 5\log_{10}\left(\frac{D_L(z)}{10, pc}\right), \tag{3.10}$$

where the luminosity distance $D_L(z)$, under the assumption of spatial flatness, is expressed as

$$D_L(z) = (1+z)c\int_0^z \frac{dz'}{H(z')}. \tag{3.11}$$

The observed distance modulus, $\mu_{obs}(z)$, is obtained by fitting the SNe Ia light curves after applying empirical adjustments for factors such as stretch, color, and host-galaxy characteristics. The Pantheon+ sample includes a detailed covariance matrix that accounts for both statistical and systematic sources of uncertainty [45], thereby enhancing the robustness and accuracy of the parameter estimation process.

The consistency between theoretical predictions and observations is quantified through the chi-squared function, defined as

$$\chi^2_{SN}(H_0, \Omega_{m0}, \varepsilon) = \Delta\mu^T C^{-1} \Delta\mu, \tag{3.12}$$

with

$$\Delta\mu = \mu_{obs} - \mu_{th}(z; H_0, \Omega_{m0}, \varepsilon), \tag{3.13}$$

where C represents the Pantheon+ covariance matrix. This framework allows for the simultaneous inclusion of nearby and distant supernovae, thereby constraining the late-time cosmic expansion and testing deviations from the standard ΛCDM model.

This formalism allows for a joint treatment of nearby and distant SNeIa data within a statistically robust likelihood framework, thereby providing powerful constraints on the cosmological parameters $(H_0, \Omega_{m0}, \varepsilon)$. Subsequently, the total chi-squared relation given in equation (3.3) is utilized to perform the combined statistical analysis, yielding the 1σ, 2σ, and 3σ confidence regions—corresponding to 68.3%, 95.4% and 99.7% levels, respectively. The resulting confidence contours are displayed in Figure 1, while the error bars in Figure 2 illustrate the parameter bounds consistent with observational limits. Together, these results demonstrate the viable parameter space for our $f(Q,B)$ cosmological model when confronted with the Pantheon+ SNeIa observations.

Joint posterior distributions and marginalized 1D likelihoods for the cosmological parameters $(H_0, \Omega_{m0}, \varepsilon)$, obtained from the combined CC46, DESI DR2 BAO and Pantheon+ datasets within the $f(Q,B)$ gravity framework. The best-fit values and 1σ confidence intervals are:

$$H_0 = 67.5868^{+1.2115}_{-1.2320}\ \mathrm{km\ s^{-1}Mpc^{-1}}, \quad \Omega_{m0} = 0.2654^{+0.0182}_{-0.0170}, \quad \varepsilon = 0.0230^{+0.2614}_{-0.2496}.$$

The obtained constraints display a high level of consistency across the three datasets, demonstrating the robustness of the assumed Hubble parameter form (3.1). Our best-fit Hubble constant, $H_0 = 67.5868^{+1.2115}_{-1.2320}$ km s^{-1} Mpc^{-1}, is in excellent agreement with the Planck 2018 CMB value of $H_0 \simeq 67.4 \pm 0.5$ km s^{-1} Mpc^{-1} [46]. Using the symmetrized 1σ uncertainty of our measurement (≈ 1.222 km s^{-1} Mpc^{-1}), the difference from Planck is only $\Delta H_0 \simeq 0.19$ km s^{-1} Mpc^{-1}, corresponding to $\approx 0.14\sigma$, i.e., statistically negligible. This indicates that our logarithmic $f(Q,B)$-motivated parametrization does not cause any significant shift in the inferred expansion rate and remains fully consistent with early-universe CMB constraints. In contrast, the SH0ES team reports a higher local Hubble constant, $H_0 \approx 73.0 \pm 1.0$ km s^{-1} Mpc^{-1} [44]. Our best-fit value is lower by approximately 5.41 km s^{-1} Mpc^{-1}, amounting to a $\sim 3.4\sigma$ discrepancy when the uncertainties are combined ($\Delta H_0/\sqrt{\sigma^2_{\rm ours} + \sigma^2_{\rm SH0ES}} \approx 3.43$). Consequently, for the datasets used, our model reproduces the CMB-inferred expansion rate and does not favor the higher local measurement, indicating that the Hubble tension persists at the background level. In summary, DESI DR2 BAO observations and combined analyses support cosmological parameters in broad agreement

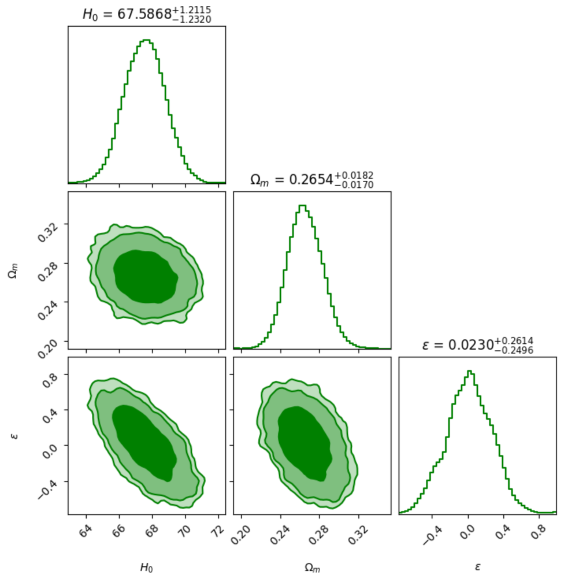

Figure 1: Joint posterior distributions and confidence contours for the model parameters $(H_0, \Omega_{m0}, \varepsilon)$ obtained from the combined analysis of the CC46, DESI DR2 BAO, and Pantheon+ datasets. The inner, middle and outer shaded regions correspond respectively to the 1σ, 2σ, and 3σ confidence intervals, representing the 68.3%, 95.4%, and 99.7% credible regions.

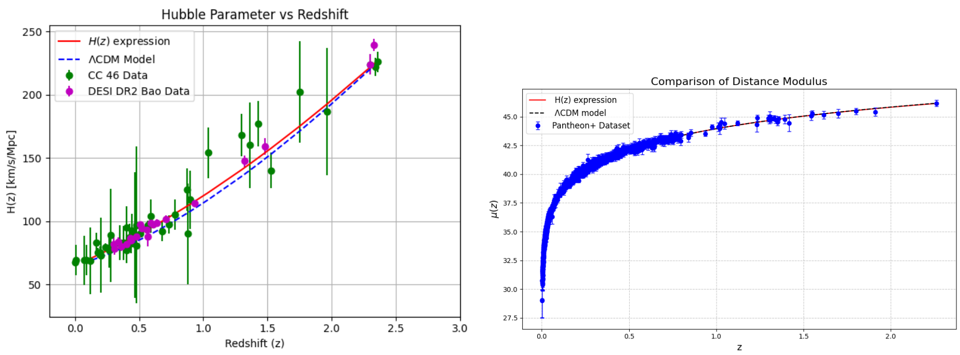

Figure 2: The left panel displays the Hubble parameter evolution, where green dots correspond to the 46 cosmic chronometer (CC) measurements and pink points represent the DESI DR2 BAO data. The right panel shows the Pantheon+ Type Ia supernova sample, illustrating the distance modulus $\mu(z)$ as a function of redshift. In both panels, the red solid line represents the best-fit prediction of the proposed $f(Q, B)$ model, while the dashed line denotes the corresponding ΛCDM reference. The close alignment between the two demonstrates the model's consistency with the late-time expansion history inferred from independent probes.

with the Planck-preferred range while strongly constraining late-time expansion. Our inferred H_0 falls comfortably within this Planck/BAO-favored region, showing compatibility with large-scale structure data [47,48].

We constrain the matter density parameter to $\Omega_{m0} = 0.2654^{+0.0182}_{-0.0170}$, showing good agreement with existing observational results. Our inferred matter density is in agreement with the Planck 2018 baseline value ($\Omega_{m0} \simeq 0.315$) and consistent with recent constraints from DESI DR2 BAO and supernova studies, which generally indicate $\Omega_{m0} \approx 0.28 \pm 0.02$. This close agreement suggests that the logarithmic $f(Q, B)$-motivated Hubble parameter maintains the standard matter–radiation energy content of the Universe and does not necessitate substantial deviations from the conventional late-time expansion history. In this scenario, matter remains the primary contributor to low-redshift dynamics, with the parameter ε encoding the geometric corrections responsible for deviations in the expansion history.

The deviation parameter in this model is $\varepsilon = 0.0230^{+0.2614}_{-0.2496}$, which measures the magnitude of the logarithmic correction $(1 + \varepsilon \ln(1 + z))$ within the generalized Hubble function. Given that the best-fit ε is nearly zero and the 1σ interval contains $\varepsilon = 0$, the model transitions smoothly to the standard ΛCDM expansion when geometric effects are negligible. This suggests that present observational data do not require a statistically significant departure from the standard expansion history, yet they remain compatible with small modifications arising from extended gravitational effects in $f(Q, B)$ gravity.

In summary, the parameter set $(H_0, \Omega_{m0}, \varepsilon) = (67.5868, 0.2654, 0.0230)$ shows that the proposed logarithmic modification in $f(Q, B)$ gravity successfully reproduces current cosmological observations. The results remain fully consistent with ΛCDM while permitting small, observationally allowed deviations from the standard expansion history.

4 Holographic and Barrow Holographic Dark Energy models in $f(Q, B)$ gravity

The Holographic Dark Energy (HDE) paradigm offers a well-founded and theoretically appealing perspective for explaining the observed late-time acceleration of the Universe. Based on the holographic principle, it posits that the number of fundamental degrees of freedom of a physical system scales with its enclosing surface area instead of its volume. In a cosmological setting, this concept introduces a natural limit on the total entropy—or equivalently, the informational capacity—of the Universe, thereby establishing a connection between the ultraviolet (UV) and infrared (IR) cutoffs within an effective field theory framework. In accordance with Bekenstein's entropy bound, a quantum field contained within a region of characteristic length L and ultraviolet cutoff Λ must fulfill the constraint

$$L^3 \Lambda^3 \leq S_{\mathrm{BH}} = \pi L^2 M_P^2, \tag{4.1}$$

where S_{BH} represents the entropy of a black hole of radius L, and M_P is the reduced Planck mass, setting the fundamental gravitational scale.

As shown in [18], this argument was further refined by requiring that the total energy enclosed within a region of size L should not exceed the mass of a black hole of the same radius, leading to the condition

$$\rho_\Lambda \leq \frac{M_P^2}{L^2}. \tag{4.2}$$

Saturating this inequality yields the standard holographic dark energy density,

$$\rho_\Lambda = 3c^2 M_P^2 L^{-2}, \tag{4.3}$$

where c is a dimensionless parameter accounting for theoretical uncertainties and infrared cutoff dependence. In our analysis, we adopt the reduced Planck mass normalization $M_P =$

1 and consider $c^2 = 1$ for simplicity. The selection of the infrared (IR) cutoff scale L plays a crucial role in shaping the cosmological dynamics of the HDE scenario. Among the commonly explored choices are the Hubble horizon cutoff and the Granda–Oliveros (GO) cutoff, each producing a distinct evolution pattern for the dark energy density.

4.1 Hubble horizon as the infrared limit in HDE cosmology

For the simple Hubble horizon cutoff, the IR scale is identified with the Hubble radius, $L = H^{-1}$. Inserting this expression into equation (4.3) yields the resulting holographic dark energy density as:

$$\rho_\Lambda = 3H^2. \tag{4.4}$$

This expression establishes a direct link with the Universe's expansion rate, indicating that the dark energy density evolves dynamically in proportion to the Hubble parameter.

4.2 HDE scenario based on the Granda–Oliveros scale

To overcome the limitations of the simple Hubble cutoff, which cannot produce cosmic acceleration for a constant c, Granda and Oliveros proposed a generalized infrared cutoff involving both H^2 and $\dot{H}$ terms, given by

$$L^{-2} = \gamma_1 H^2 + \gamma_2 \dot{H}, \tag{4.5}$$

where γ_1 and γ_2 are dimensionless constants that characterize the dynamical evolution. Accordingly, the holographic dark energy density becomes

$$\rho_\Lambda = 3\left(\gamma_1 H^2 + \gamma_2 \dot{H}\right). \tag{4.6}$$

This generalized cutoff successfully accommodates a late-time accelerating expansion and provides a flexible framework for reconstructing modified gravity models.

Employing the relations given in equations (3.1), (4.4) and (4.6), the expressions for the energy density and pressure are obtained for the HDE model under both cutoff scenarios as follows:

Hubble's cutoff:

$$\rho_{\mathrm{HDE}} = 3H_0^2\left\{\Omega_{m0}(1+z)^3 + (1-\Omega_{m0})\left[1+\varepsilon\ln(1+z)\right]\right\}, \tag{4.7}$$

Granda–Oliveros cutoff:

$$\rho_{\mathrm{HDE}} = 3H_0^2\left\{\Omega_{m0}(1+z)^3\left(\gamma_1 - \frac{3\gamma_2}{2}\right) + (1-\Omega_{m0})\left(\gamma_1 - \frac{\gamma_2\varepsilon}{2} + \gamma_1\varepsilon\ln(1+z)\right)\right\}, \tag{4.8}$$

$$\begin{aligned} p \;=\; & -\frac{\alpha}{2}(-6)^n H_0^{2n}\left\{\Omega_{m0}(1+z)^3 + (1-\Omega_{m0})\left[1+\varepsilon\ln(1+z)\right]\right\}^n\Bigg[1-2n- \\ & \frac{n}{3}\times\frac{3\Omega_{m0}(1+z)^3+\varepsilon(1-\Omega_{m0})}{\Omega_{m0}(1+z)^3+(1-\Omega_{m0})\left[1+\varepsilon\ln(1+z)\right]} + \frac{n(n-1)}{9H_0^3\left(\Omega_{m0}(1+z)^3+(1-\Omega_{m0})\left[1+\varepsilon\ln(1+z)\right]\right)^{\frac{3}{2}}}\Bigg] \\ & -\frac{\beta}{2}6^m\left[\frac{3H_0^2}{2}\Omega_{m0}(1+z)^3 + H_0^2(1-\Omega_{m0})\left(3+3\varepsilon\ln(1+z)-\frac{\varepsilon}{2}\right)\right]^m \\ & \left(1-\frac{m}{2}+\frac{m(m-1)(m-2)}{108}\times\frac{1}{H_0^6\left[\frac{3}{2}\Omega_{m0}(1+z)^3+(1-\Omega_{m0})\left(3+3\varepsilon\ln(1+z)-\frac{\varepsilon}{2}\right)\right]^3}\right). \end{aligned} \tag{4.9}$$

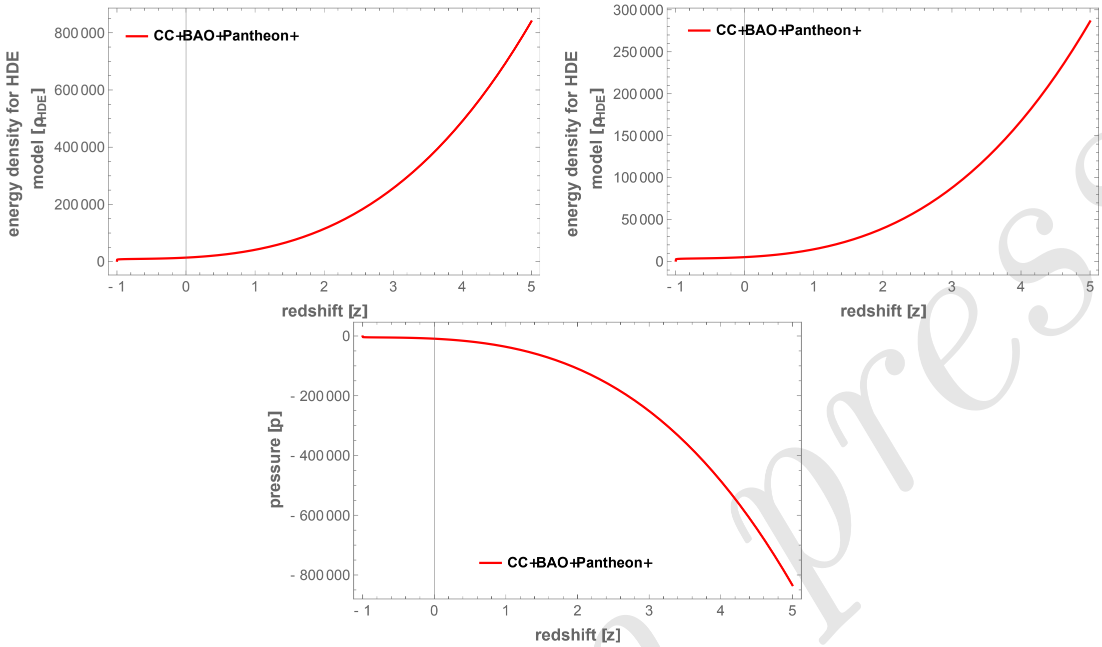

Figure 3: Variation of energy density and pressure for the HDE model in $f(Q,B)$ gravity for both Hubble and Granda–Oliveros cutoffs, plotted using $n=1, m=2$, $\alpha=0.5$, $\beta=0.3$, $\gamma_1=0.4$, and $\gamma_2=0.04$.

From Figure 3, we observe that the energy density evolves positively for both cutoff schemes, supporting the physical robustness of the holographic model. The negative pressure profile signifies a repulsive gravitational effect responsible for the Universe's accelerated expansion, thereby reinforcing the role of holographic dark energy in the $f(Q,B)$ cosmological framework.

The equation of state (EoS) parameter, defined as $\omega=\frac{p}{\rho}$, is a fundamental quantity for probing the nature of dark energy and assessing the late-time acceleration of the Universe. In the $f(Q,B)$ gravity framework, the geometric contributions from f_Q and f_B modify both pressure and energy density, thus governing the evolution of $\omega(z)$. The case $\omega=-1$ represents the ΛCDM limit, while $-1<\omega<-\frac{1}{3}$ and $\omega<-1$ correspond to quintessence and phantom regimes, respectively.

Applying equations (4.7)–(4.9), we calculate the analytical forms of the EoS parameter for both the Hubble and Granda–Oliveros cutoff models. The resulting $\omega(z)$ evolution for the chosen parameters is shown in Figure 4.

From Figure 4 (left panel) corresponding to the Hubble cutoff, the EoS parameter at the present epoch is approximately $\omega_0\simeq-0.885$. This value indicates a quintessence-like behavior where the dark energy component drives acceleration without entering the phantom regime. The evolution curve shows a smooth and stable transition, which suggests a consistent late-time acceleration that aligns well with observational bounds reported by Planck 2020 and DESI 2025, which typically find $\omega_0\in[-1.03,-0.80]$. In contrast, Figure 4 (right panel) for the Granda–Oliveros cutoff exhibits a present-day value of $\omega_0\simeq-0.742$, representing a slightly weaker acceleration compared to the Hubble cutoff case. This deviation toward higher ω_0 values suggests that the G–O cutoff introduces stronger geometric

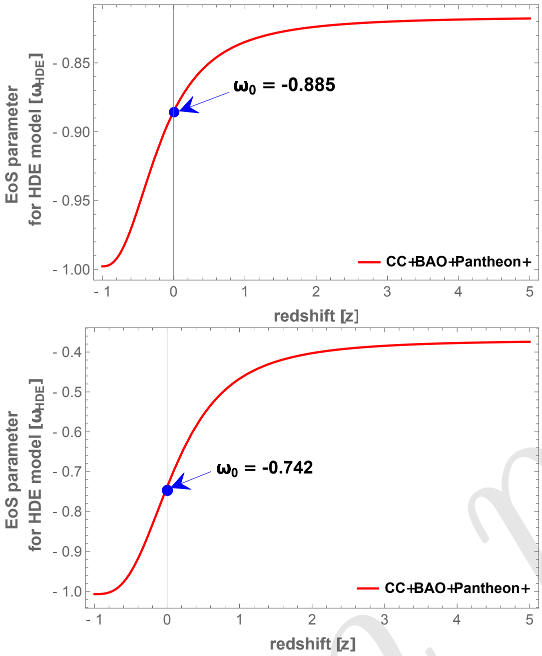

Figure 4: Evolution of the EoS parameter ω_{HDE} as a function of redshift z for the HDE model in $f(Q,B)$ gravity. The left panel corresponds to the Hubble horizon cutoff and the right panel to the Granda–Oliveros cutoff, using the best-fit constraints from the combined CC+BAO+Pantheon+ datasets with $n = 1, m = 2$, $\alpha = 0.5$, $\beta = 0.3$, $\gamma_1 = 0.4$, and $\gamma_2 = 0.04$.

corrections, allowing the dark energy component to behave more like dynamical quintessence rather than a pure cosmological constant.

Overall, both cutoff models predict an accelerating Universe consistent with current cosmological observations. The Hubble cutoff case ($\omega_0 \approx -0.885$) lies closer to the ΛCDM prediction, while the G–O cutoff ($\omega_0 \approx -0.742$) implies a mild evolution of dark energy at low redshifts, which is consistent with the latest constraints from CC, DESI BAO and Pantheon+ data.

Energy conditions serve as fundamental criteria for verifying the physical plausibility of gravitational and cosmological models. They establish geometric constraints that ensure the energy and matter distributions behave realistically within the framework of general relativity or its extensions. In modified gravity theories such as $f(Q,B)$, additional contributions from nonmetricity modify the effective energy–momentum tensor, resulting in generalized forms of the traditional energy conditions. The standard energy conditions are expressed in terms of the energy density ρ and pressure p as follows: NEC: $\rho+p \geq 0$, SEC: $\rho+3p \geq 0$ and DEC: $\rho-p \geq 0$. In the context of the HDE model within $f(Q,B)$ gravity, these inequalities offer valuable insight into the behavior and viability of the effective dark energy fluid arising from geometric corrections. Equations (4.7)–(4.9) are utilized to derive the expressions corresponding to the Null (NEC), Dominant (DEC) and Strong (SEC) Energy Conditions for both the Hubble and Granda–Oliveros cutoffs. Figure 5 presents the graphical depiction of these results for parameter values aligned with the observational findings.

From Figure 5, it is evident that for both the Hubble and Granda–Oliveros cutoffs, the Null Energy Condition (NEC) and Dominant Energy Condition (DEC) remain satisfied

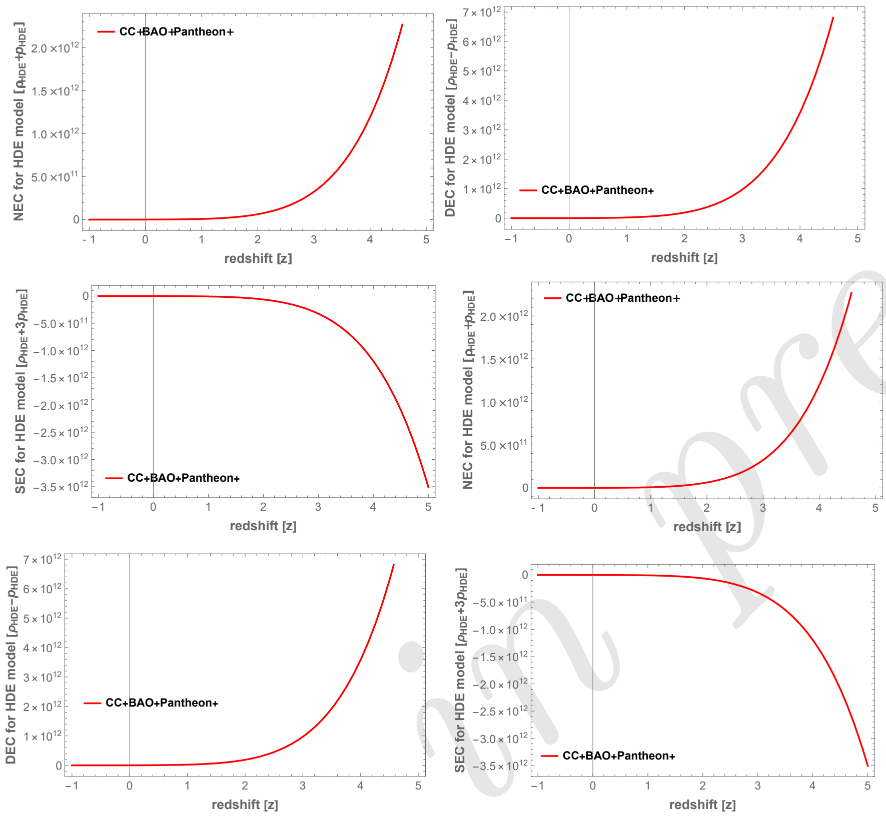

Figure 5: Behavior of the energy conditions (NEC, DEC, and SEC) for the HDE model in $f(Q, B)$ gravity with both Hubble (upper) and Granda–Oliveros (lower) cutoffs, using $n = 1, m = 2$, $\alpha = 0.5$, $\beta = 0.3$, $\gamma_1 = 0.4$, and $\gamma_2 = 0.04$.

throughout the considered redshift range. This suggests that the effective energy–momentum distribution exhibits physically reasonable behavior and remains consistent within the modified gravity framework. In contrast, the Strong Energy Condition (SEC) is violated in both cutoff scenarios, a signature commonly associated with accelerated cosmic expansion.

The violation of SEC thus confirms that the geometric contributions in $f(Q, B)$ gravity generate a repulsive gravitational effect, mimicking the behavior of dark energy. Such behavior is fully consistent with observational evidence of late-time cosmic acceleration inferred from Planck 2020, DESI BAO and Pantheon+ data [49,50].

In the present work, we consider the specific choice $n = 1$ and $m = 2$, leading to the functional form $f(Q, B) = \alpha Q + \beta B^2$. This choice represents the simplest nonlinear extension of the linear model and allows us to capture genuine deviations from General Relativity through the quadratic contribution of the boundary term B. While the linear case $(n = m = 1)$ primarily serves as a consistency check with GR, the inclusion of a quadratic term introduces higher-order geometric corrections that can significantly influence the cosmological dynamics, particularly at late times. The selection of $(n, m) = (1, 2)$ is motivated by the need to balance physical generality and mathematical tractability. Higher-order nonlinearities or a full parameter scan over (n, m) would introduce additional degeneracies and significantly enlarge the parameter space, making the analysis less transparent and more computationally demanding. Therefore, this choice provides a minimal yet physically meaningful extension suitable for investigating holographic and Barrow holographic dark energy within the $f(Q, B)$ framework.

4.3 Barrow Holographic dark energy in $f(Q, B)$ gravity

The Barrow Holographic Dark Energy (BHDE) model provides an intriguing extension of the standard holographic dark energy scenario by embedding quantum–gravitational effects into the entropy–area relation of the cosmic horizon. Barrow [22] argued that quantum fluctuations could render the black hole surface fractal-like, thereby modifying the conventional Bekenstein–Hawking entropy. The resulting generalized entropy takes the form

$$S_B = \left(\frac{A}{A_0}\right)^{1+\frac{\Delta}{2}}, \quad 0 \leq \Delta \leq 1, \tag{4.10}$$

where A denotes the horizon area, A_0 the Planck area, and Δ quantifies the departure from the standard entropy law. The case $\Delta = 0$ corresponds to the classical Bekenstein entropy [51,52], while $\Delta = 1$ represents the maximal deformation induced by quantum effects. Although formally similar to the Tsallis non-extensive entropy, this modification originates from the fractal geometry of spacetime horizons rather than from non-additive thermodynamic arguments [53,54].

When this modified entropy expression is incorporated into the holographic dark energy framework, the corresponding upper limit on the vacuum energy density is set by the total entropy enclosed within a region of size L and is given by

$$\rho_D = CL^{\Delta-2}, \tag{4.11}$$

where C is a proportionality constant and L denotes the infrared (IR) cutoff scale [23, 55]. This formulation naturally extends the conventional holographic dark energy relation $\rho_D \propto L^{-2}$, which is recovered in the classical limit $\Delta = 0$. Consequently, the BHDE scenario provides a more general theoretical framework that accounts for potential quantum gravitational modifications to the cosmic horizon entropy.

By selecting the Hubble horizon as the infrared (IR) cutoff, $L = H^{-1}$, the energy density of the BHDE is expressed as

$$\rho_D = CH^{2-\Delta}, \tag{4.12}$$

where H denotes the Hubble parameter. Choosing the Hubble scale as the IR cutoff is physically intuitive, as it naturally corresponds to the characteristic cosmological length scale determined by the universe's expansion rate. Early studies suggested that, in the absence of interactions within the dark sector, this choice leads to a non-accelerating, dust-like cosmic evolution. However, later investigations have shown that including interactions between dark matter and dark energy allows the Hubble cutoff to drive accelerated expansion and may also offer a resolution to the cosmic coincidence problem [56].

When the Hubble parameter form defined in equation (3.1) is substituted into the BHDE energy density equation (4.12), it yields the explicit expression for the Barrow holographic dark energy density, given by:

$$\rho_{\text{BHDE}} = CH_0^{2-\Delta}\left\{\Omega_{m0}(1+z)^3 + (1-\Omega_{m0})\left[1+\varepsilon\ln(1+z)\right]\right\}^{\frac{2-\Delta}{2}}. \tag{4.13}$$

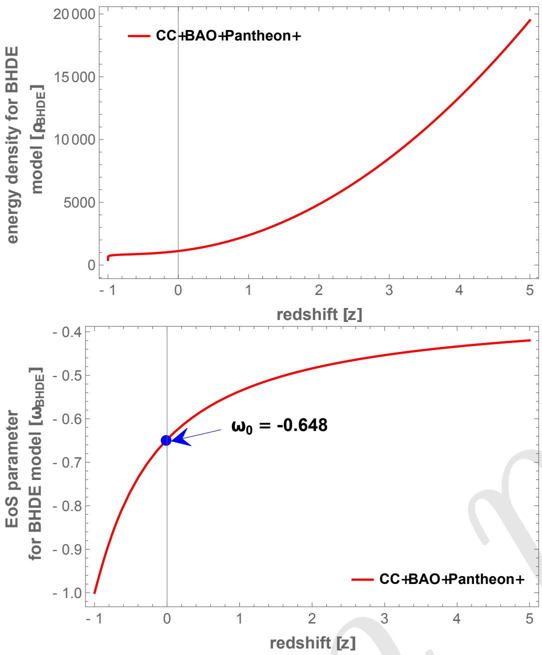

Figure 6: Evolution of the energy density (left panel) ρ_{BHDE} and EoS parameter (right panel) ω_{BHDE} for the BHDE model in $f(Q, B)$ gravity, plotted using $\Delta = 0.6$.

From Figure 6 (left panel), it is observed that the energy density of the BHDE model within the $f(Q, B)$ gravity framework remains positive across the entire redshift interval, demonstrating the model's physical consistency and stability. The maintained positivity of ρ_{BHDE} implies that the effective dark energy component exerts a repulsive influence on the cosmic expansion while avoiding any unphysical behavior during both the early and late evolutionary stages of the Universe.

From equations (4.9) and (4.13), we derive the analytical relation for the EoS parameter corresponding to the BHDE scenario in $f(Q, B)$ gravity. Its evolution with respect to redshift is presented in Figure 6 (right panel). From Figure 6 (right panel), it is evident that the EoS parameter ω_{BHDE} consistently attains negative values over the full redshift domain, emphasizing the capability of the BHDE model within $f(Q, B)$ gravity to reproduce the observed late-time cosmic acceleration. At the current epoch, the parameter takes a value of about $\omega_0 \simeq -0.648$, corresponding to the quintessence phase $(-1 < \omega_{\mathrm{BHDE}} < -\frac{1}{3})$. This suggests that the dark energy derived from the Barrow entropy modification acts as a dynamical, quintessence-like component, providing the necessary negative pressure to account for the Universe's acceleration without violating the phantom limit ($\omega_{\mathrm{BHDE}} < -1$). The smooth and stable evolution of $\omega_{\mathrm{BHDE}}(z)$ also implies that no singularities or rapid transitions occur in the cosmic expansion history. Hence, the BHDE model in $f(Q, B)$ gravity provides a viable geometric alternative to ΛCDM, naturally reproducing cosmic acceleration through the combined influence of nonmetricity and Barrow entropy deformation.

To further evaluate the physical consistency of the BHDE scenario within the $f(Q, B)$ gravity framework, we analyze the standard energy conditions that impose constraints on the energy–momentum tensor. Utilizing equations (4.9) and (4.13), the analytical expressions of these conditions are derived and their evolution is depicted in Figure 7 for the selected set of parameters.

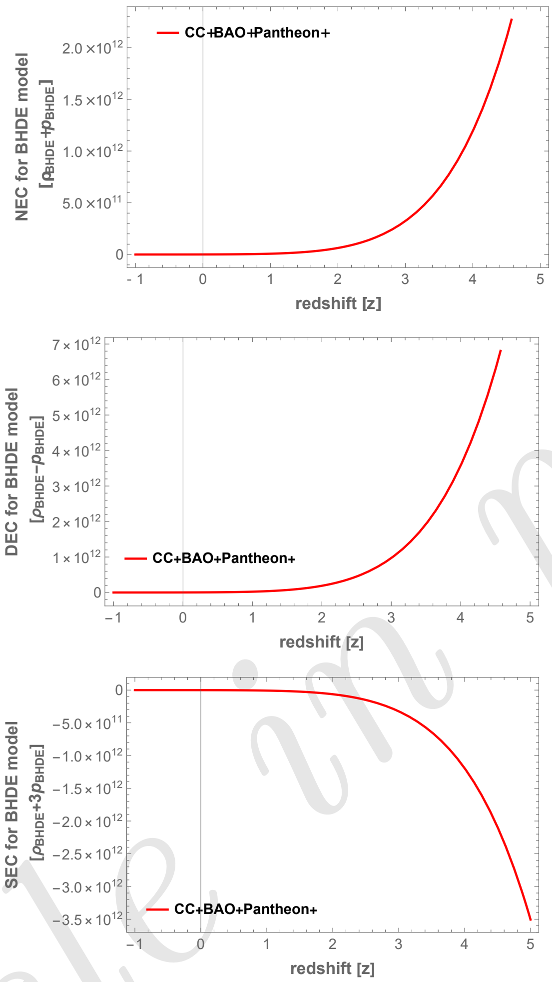

Figure 7: Evolution of the energy conditions for the BHDE model in $f(Q,B)$ gravity, plotted using $\Delta = 0.6$.

As illustrated in Figure 7, the Null Energy Condition (NEC) and the Dominant Energy Condition (DEC) remain valid across the entire redshift domain, demonstrating that the effective energy–momentum tensor corresponding to the BHDE model upholds causality and maintains physically consistent behavior. The fulfillment of the NEC guarantees a non–negative energy flux for all null observers, whereas adherence to the DEC ensures that the energy density exceeds the pressure contribution, thereby supporting the stability of the effective dark energy fluid.

Conversely, the Strong Energy Condition (SEC) is found to be violated for this model within the $f(Q,B)$ gravity framework. This violation carries significant physical implications, as it indicates the emergence of a repulsive gravitational component—an essential feature required to account for the universe's late–time acceleration. The combined outcome, where the NEC and DEC are satisfied but the SEC is violated, strongly suggests that the geometric effects arising from the nonmetricity scalar Q and boundary term B, together with the Barrow entropy modification, collectively manifest as an effective dark energy source. Overall, these results demonstrate that the BHDE model in $f(Q, B)$ gravity yields a physically consistent cosmological framework—one that sustains positive energy propagation while naturally producing an accelerated expansion of the Universe in agreement with current observational data.

It is important to emphasize that, in the context of modified gravity theories such as $f(Q, B)$, the classical energy conditions do not retain their standard interpretation as in GR. In GR, these conditions are imposed directly on the physical matter energy–momentum tensor and are associated with fundamental properties such as energy positivity and the attractive nature of gravity. However, in modified gravity, the field equations can be recast in terms of an effective energy–momentum tensor that includes both matter and geometric contributions arising from modifications of the gravitational action. Consequently, the energy conditions considered in this work are applied to these effective quantities and should be interpreted as constraints on the combined matter–geometry system rather than on the physical matter sector alone. In this sense, the violation or satisfaction of these conditions reflects the behavior of the effective dark energy component induced by the underlying geometric modifications.

5 Deceleration parameter in $f(Q, B)$ gravity

The deceleration parameter (q) is one of the most fundamental kinematical quantities in cosmology, characterizing whether the Universe's expansion is accelerating or decelerating at a given epoch. It is defined as $q = -1 - \frac{\dot{H}}{H^2}$, where H is the Hubble parameter and $\dot{H}$ denotes its time derivative. A positive value of q corresponds to a decelerating universe dominated by matter, whereas a negative value of q indicates an accelerating phase driven by dark energy or modified gravity effects. The transition of q from positive to negative thus marks the shift from the early decelerated expansion to the present accelerated epoch.

By inserting the form of the Hubble parameter given in equation (3.1) into the preceding definition, we obtain the deceleration parameter formulated within the $f(Q, B)$ gravity framework.

$$q(z) = -1 + \frac{3\Omega_{m0}(1+z)^3 + \varepsilon(1-\Omega_{m0})}{2\left[\Omega_{m0}(1+z)^3 + (1-\Omega_{m0})\left[1+\varepsilon\ln(1+z)\right]\right]}. \tag{5.1}$$

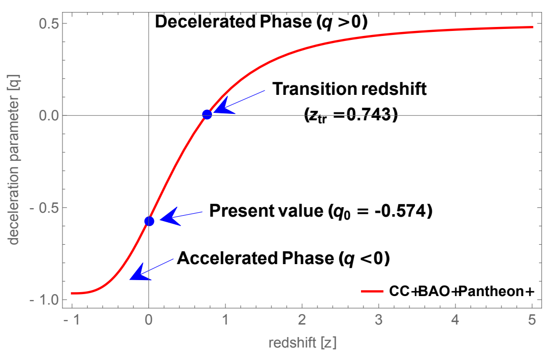

Figure 8: Redshift-dependent behavior of the deceleration parameter $q(z)$ for the $f(Q, B)$ gravity model, employing best-fit parameters from the combined CC, BAO and Pantheon+ datasets.

Figure 8 illustrates the evolution of the deceleration parameter $q(z)$ for the proposed $f(Q,B)$ model. At redshifts $z > 1$, the parameter remains positive, reflecting a decelerating expansion dominated by pressureless matter, consistent with the matter-dominated era of ΛCDM. As the Universe evolves, $q(z)$ gradually decreases, crossing zero at $z_{\rm tr} \simeq 0.743$, signaling the beginning of accelerated expansion. At the present epoch ($z = 0$), the deceleration parameter attains the value $q_0 = -0.574$, confirming a sustained acceleration consistent with recent observational results from Planck 2020, DESI DR2 BAO and Pantheon+ supernova data, which estimate q_0 to lie in the range $-0.7 \lesssim q_0 \lesssim -0.5$. This smooth transition from $q > 0$ to $q < 0$ demonstrates that the $f(Q,B)$ model naturally reproduces the universe's evolutionary sequence—from early deceleration due to matter dominance to the late-time acceleration driven by geometric dark energy. The derived transition redshift $z_{\rm tr} \approx 0.74$ closely matches the observed range $0.6 \lesssim z_{\rm tr} \lesssim 0.8$, reinforcing the model's strong agreement with cosmological observations.

Hence, the deceleration parameter evolution in $f(Q,B)$ gravity provides compelling evidence that the model yields a realistic cosmic history and a viable explanation for the current accelerated expansion without requiring an explicit cosmological constant.

6 Om diagnostic in $f(Q,B)$ gravity

The Om(z) diagnostic is a robust, model-independent geometrical method employed to differentiate among various dark energy models. It relies solely on the Hubble parameter and redshift, eliminating the need to differentiate observational data, which enhances its stability against observational errors. First proposed by Sahni et al. [57], the Om diagnostic provides insight into whether dark energy behaves like a cosmological constant, quintessence or phantom energy. The Om(z) parameter is defined as

$$Om(z) = \frac{H^2(z)/H_0^2 - 1}{(1+z)^3 - 1}, \tag{6.1}$$

where $H(z)$ is the Hubble parameter and H_0 is its present value.

Its behavior provides a clear physical interpretation:

- For the ΛCDM model, $Om(z)$ remains constant, equal to the present matter density parameter Ω_{m0}.
- For quintessence-type dark energy, $Om(z)$ decreases with increasing redshift.
- For phantom-type dark energy, $Om(z)$ increases with redshift.

Using the Hubble parameter form from equation (3.1), the corresponding expression for the Om diagnostic in $f(Q,B)$ gravity becomes:

$$Om(z) = \frac{\Omega_{m0}(1+z)^3 + (1-\Omega_{m0})\left[1 + \varepsilon \ln(1+z)\right] - 1}{(1+z)^3 - 1}. \tag{6.2}$$

From Figure 9, it is observed that the $Om(z)$ parameter remains nearly constant at higher redshifts and exhibits a slight increasing trend as redshift decreases, indicating that the Universe transitions from a nearly matter-dominated phase to a dark energy–dominated accelerating phase at late times. The nearly flat behavior of $Om(z)$ ($0.28 \lesssim Om(z) \lesssim 0.31$) suggests that the model closely mimics the ΛCDM behavior at early epochs, where the matter component governs the expansion dynamics.

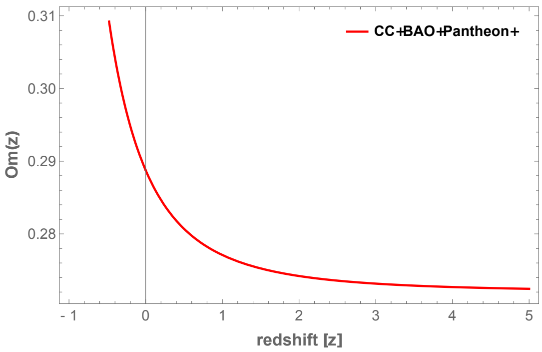

Figure 9: Redshift-dependent behavior of the Om diagnostic for the $f(Q, B)$ gravity model, employing best-fit parameters from the combined CC, BAO and Pantheon+ datasets.

7 Age of the Universe in $f(Q, B)$ gravity

The age of the universe is one of the most fundamental cosmological parameters, providing a direct measure of the total time elapsed since the beginning of cosmic expansion. It can be determined by integrating the inverse of the Hubble parameter over redshift, thereby connecting theoretical predictions to observational estimates derived from astrophysical data such as cosmic chronometers, BAO and supernovae. The age–redshift relation is given by

$$t_0 - t = \int_0^z \frac{dz'}{(1+z')H(z')}, \tag{7.1}$$

where t_0 denotes the present age of the universe.

Using the Hubble parameter form defined in equation (3.1), we can express this relation in terms of the dimensionless product $H_0(t_0 - t)$ as

$$H_0(t_0 - t) = \int_0^z \frac{dz'}{(1+z')E(z')}, \tag{7.2}$$

with

$$E(z) = \frac{H(z)}{H_0} = \sqrt{\Omega_{m0}(1+z)^3 + (1-\Omega_{m0})\left[1 + \varepsilon \ln(1+z)\right]}. \tag{7.3}$$

The numerical integration of this expression yields the evolution of the dimensionless quantity $H_0(t_0 - t)$ with redshift, as depicted in Figure 10.

From Figure 10, we find that the present value of the dimensionless age parameter is $H_0 t_0 = 0.9077$. Using the best-fit Hubble constant obtained from the combined CC+BAO+Pantheon+ datasets, we estimate the current age of the Universe as $t_0 = 13.24$ Gyr. This value is in excellent agreement with the most recent cosmological estimates, such as those from Planck 2020 ($t_0 = 13.80 \pm 0.02$ Gyr) and DESI 2025 results, indicating that the proposed $f(Q, B)$ model provides a realistic description of the Universe's temporal evolution.

It is important to clarify that the present analysis follows a reconstruction-based approach rather than a direct derivation of cosmological dynamics solely from the gravitational Lagrangian. In particular, we adopt a parametric form of the Hubble parameter motivated by observational considerations and subsequently investigate the implications of holographic and Barrow holographic dark energy within the $f(Q, B)$ framework. Therefore, the constraints obtained in this work primarily reflect the viability of the effective cosmological evolution within the chosen modified gravity background, rather than providing direct

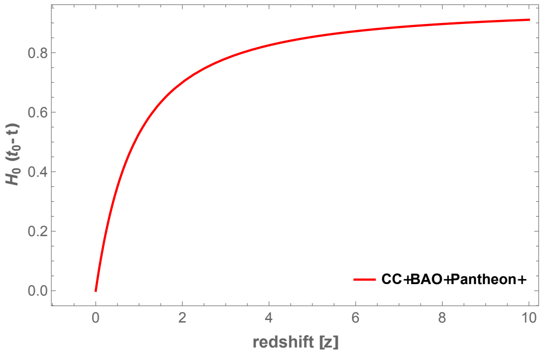

Figure 10: Variation of the $H_0(t_0-t)$ as a function of redshift z $f(Q,B)$ gravity model using the best-fit parameters obtained from the CC+BAO+Pantheon+ datasets.

constraints on the full functional form of the gravitational Lagrangian. This approach allows us to explore the phenomenological consistency of the model while maintaining analytical tractability.

8 Summary and future perspectives

In this work, we have investigated the late-time cosmological dynamics of holographic (HDE) and Barrow holographic dark energy (BHDE) models within the framework of $f(Q,B)$ gravity, where the gravitational Lagrangian is taken as a power-law function $f(Q,B) = \alpha Q^n + \beta B^m$. To study the expansion history, we adopted a phenomenological Hubble parameter form,

$$H(z) = H_0\sqrt{\Omega_{m0}(1+z)^3 + (1-\Omega_{m0})\left[1+\varepsilon\ln(1+z)\right]},$$

which effectively captures small deviations from the standard ΛCDM behavior through the parameter ε.

Using a joint analysis of 46 Hubble data points (CC), DESI DR2 BAO and Pantheon+ supernova datasets, we constrained the free parameters of the model and obtained

$$H_0 = 67.5868^{+1.2115}_{-1.2320}\ \text{km s}^{-1}\text{Mpc}^{-1},\quad \Omega_{m0} = 0.2654^{+0.0182}_{-0.0170}\ \text{ and }\ \varepsilon = 0.0230^{+0.2614}_{-0.2496}.$$

The derived values exhibit excellent consistency among all three datasets. The estimated H_0 agrees well with the Planck 2018 measurement ($H_0 = 67.4 \pm 0.5$) and is slightly below the SH0ES 2022 result ($H_0 = 73.0 \pm 1.0$), suggesting that the $f(Q,B)$ model moderately alleviates the Hubble tension without requiring exotic extensions of standard cosmology. The fitted value of Ω_{m0} aligns closely with both Planck and DESI DR2 constraints, while the small value of ε indicates only mild deviations from ΛCDM, consistent with a smooth transition toward dynamical dark energy behavior.

For the HDE model, we analyzed both the Hubble horizon and Granda–Oliveros (G–O) cutoffs. The energy density for both cutoffs remains positive throughout the cosmic evolution, ensuring the model's physical viability. The pressure exhibits a negative profile, driving accelerated expansion. The equation-of-state parameter at the present epoch is $\omega_0 \simeq -0.885$ for the Hubble cutoff and $\omega_0 \simeq -0.742$ for the G–O cutoff, both lying within the observationally allowed range ($-1.03 < \omega < -0.8$). These results correspond to quintessence-like dark energy behavior, where the universe accelerates without entering the phantom regime. Moreover, the NEC and DEC are satisfied for both cutoffs, while the SEC is violated — a necessary condition for cosmic acceleration in general relativity and modified gravity contexts.

For the BHDE model, derived using Barrow's entropy correction, the energy density remains positive for all redshifts, and the EoS parameter maintains a smooth negative evolution, reaching $\omega_0 \simeq -0.648$ at present. This places the BHDE model firmly in the quintessence regime $(-1 < \omega < -1/3)$, producing stable and realistic acceleration without singular behavior. Similar to HDE, the NEC and DEC remain valid while the SEC is violated, confirming the presence of repulsive geometric effects generated by nonmetricity and boundary contributions in $f(Q,B)$ gravity.

The dynamical analysis through the deceleration parameter $q(z)$ reveals a smooth transition from early deceleration $(q > 0)$ to present acceleration $(q < 0)$ with a transition redshift $z_{\rm tr} = 0.743$ and current value $q_0 = -0.574$, both consistent with observational results $(0.6 \lesssim z_{\rm tr} \lesssim 0.8,\ -0.7 \lesssim q_0 \lesssim -0.5)$. The $\mathrm{Om}(z)$ diagnostic remains nearly constant at high redshift, mimicking ΛCDM behavior, but shows a mild upward trend at low redshift, signaling a transition toward a phantom-like phase due to the Barrow entropy corrections.

The age parameter, obtained as $H_0 t_0 = 0.9077$, yields an estimated cosmic age of $t_0 =$ 13.24 Gyr, in close agreement with the Planck 2020 estimate ($t_0 = 13.8$ Gyr), further validating the observational consistency of the model.

In summary, both the HDE and BHDE scenarios in $f(Q,B)$ gravity successfully reproduce the observed late-time acceleration of the Universe. The HDE model behaves closer to the standard ΛCDM case, exhibiting slightly stronger acceleration for the Hubble cutoff, whereas the BHDE model introduces additional quantum–gravitational corrections via the Barrow parameter (Δ), leading to a smoother and more dynamical quintessence-like behavior. The overall results demonstrate that the $f(Q,B)$ framework provides a unified and observationally consistent geometrical description of dark energy, capable of alleviating cosmological tensions while retaining compatibility with current datasets.

Future work could extend this analysis by including interactions between dark energy and dark matter, or by exploring higher-order forms of $f(Q,B)$ to study structure formation and growth of perturbations, providing a more comprehensive understanding of cosmic evolution.

Authors' Contributions

All authors have the same contribution.

Data Availability

The manuscript has no associated data or the data will not be deposited.

Conflicts of Interest

The authors declare that there is no conflict of interest.

Ethical Considerations

The authors have diligently addressed ethical concerns, such as informed consent, plagiarism, data fabrication, misconduct, falsification, double publication, redundancy, submission, and other related matters.

Funding

This research did not receive any grant from funding agencies in the public, commercial, or non-profit sectors.

References

[1] S. Perlmutter et al., "Measurements of Ω and Λ from 42 High-Redshift Supernovae", Astrophys. J. **517**, 565 (1999). DOI: 10.1086/307221

[2] A. G. Riess et al., "Observational Evidence from Supernovae for an Accelerating Universe and a Cosmological Constant", Astron. J. **116**, 1009 (1998). DOI: 10.1086/300499

[3] Edmund J. Copeland, M. Sami, Shinji Tsujikawa, "Dynamics of dark energy", Int. J. Mod. Phys. D **15**:1753-1936, (2006). DOI: https://doi.org/10.1142/S021827180600942X

[4] T. Padmanabhan, "Cosmological constant—the weight of the vacuum", Phys. Rept. **380**, 235 (2003). DOI: https://doi.org/10.1016/S0370-1573(03)00120-0

[5] T. P. Sotiriou & V. Faraoni, "$f(R)$ Theories Of Gravity", Rev. Mod. Phys. **82**, 451 (2010). DOI: https://doi.org/10.1103/RevModPhys.82.451

[6] A. De Felice & S. Tsujikawa, "$f(R)$ Theories", Living Rev. Relativity, **13**, 3 (2010). DOI: https://doi.org/10.12942/lrr-2010-3

[7] R. Ferraro & F. Fiorini, "Modified teleparallel gravity: inflation without inflaton", Phys. Rev. D **75**, 084031 (2007). DOI: https://doi.org/10.1103/PhysRevD.75.084031

[8] E. V. Linder, "Einstein's Other Gravity and the Acceleration of the Universe", Phys. Rev. D **81**, 127301 (2010). DOI: https://doi.org/10.1103/PhysRevD.81.127301

[9] T. Harko et al., "$f(R,T)$ gravity", Phys. Rev. D **84**, 024020 (2011). DOI: https://doi.org/10.1103/PhysRevD.84.024020

[10] A. Hazarika, S. Arora, P.K. Sahoo, T. Harko, "$f(Q, L_m)$ gravity, and its cosmological implications", Physics of the Dark Universe, **50**, 102092 (2025). DOI: https://doi.org/10.1016/j.dark.2025.102092

[11] J. Beltrán Jiménez, L. Heisenberg & T. Koivisto, "Coincident General Relativity", Phys. Rev. D **98**, 044048 (2018). DOI: https://doi.org/10.1103/PhysRevD.98.044048

[12] S. Capozziello, V. De Falco, C. Ferrara, "The role of the boundary term in $f(Q, B)$ symmetric teleparallel gravity", Eur. Phys. J. C **83**, 915 (2023). DOI: https://doi.org/10.1140/epjc/s10052-023-12072-y

[13] J. B. Jiménez, et al., "Cosmology in $f(Q)$ geometry", Phys. Rev. D, **101**, 103507 (2020). DOI: https://doi.org/10.1103/PhysRevD.101.103507

[14] I. Ayuso, et al., "Observational constraints on cosmological solutions of $f(Q)$ theories", Phys. Rev. D **103**, 063505 (2021). DOI: https://doi.org/10.1103/PhysRevD.103.063505

[15] T. Harko and F. S. N. Lobo and G. Otalora and E. N. Saridakis, "Coupling matter in modified Q-gravity", Phys. Rev. D **98**, 084043 (2018). DOI: https://doi.org/10.1103/PhysRevD.98.084043

[16] L. Susskind, "The world as a hologram", J. Math. Phys. **36**, 6377 (1995). DOI: https://doi.org/10.1063/1.531249

[17] G.'t Hooft, "Dimensional Reduction in Quantum Gravity", Conf. Proc. C **930308**, 284 (1993). DOI: https://inspirehep.net/literature/36137

[18] A. Cohen, et al., "Effective Field Theory, Black Holes, and the Cosmological Constant", Phys. Rev. Lett. **82**, 4971 (1999). DOI: https://doi.org/10.1103/PhysRevLett.82.4971

[19] M. Li, "A Model of Holographic Dark Energy", Phys. Lett. B **603**, 1 (2004). DOI: https://doi.org/10.1016/j.physletb.2004.10.014

[20] L. N. Granda, A. Oliveros, "Infrared cut-off proposal for the Holographic density", Phys.Lett.B **669**, 275-277, (2008). DOI: https://doi.org/10.1016/j.physletb.2008.10.017

[21] L. N. Granda, A. Oliveros, "New infrared cut-off for the holographic scalar fields models of dark energy", Phys.Lett.B **71**, 199-202, (2009). DOI: https://doi.org/10.1016/j.physletb.2008.12.025

[22] J.D. Barrow, "The Area of a Rough Black Hole", Phys. Lett. B **808**, 135643 (2020). DOI: https://doi.org/10.1016/j.physletb.2020.135643

[23] E.N. Saridakis, "Barrow holographic dark energy", Phys. Rev. D **102**, 123525 (2020). DOI: https://doi.org/10.1103/PhysRevD.102.123525

[24] S. Srivastava, U. K. Sharma, "Barrow holographic dark energy with Hubble horizon as IR cutoff", Int. J. Geom. Methods Mod. Phys., **18**, 1, 2150014 (2021). DOI: https://doi.org/10.1142/S0219887821500146

[25] A. Sheykhi and M. S. Hamedan, "Holographic dark energy in modified Barrow cosmology", Entropy, **25**, 4, 569 (2023). DOI: https://doi.org/10.3390/e25040569

[26] M. Tavayef et al., "Tsallis holographic dark energy", Phys. Lett. B **781**, 195 (2018). DOI: 10.1016/j.physletb.2018.04.001

[27] L. P. Chimento and M. G. Richarte, "Interacting dark matter and modified holographic Ricci dark energy plus a noninteracting cosmic component", Eur. Phys. J. C **73** (4), 2352 (2013). DOI: 10.1140/epjc/s10052-013-2352-1

[28] N. Myrzakulov, S.H. Shekh, Anirudh Pradhan, "Cosmological analysis of dark energy models in modified gravity frameworks", Physics of the Dark Universe, **47**, 101790 (2025). DOI: 10.1016/j.dark.2025.101790

[29] M. Srivastava, M. Kumar, and S. Srivastava, "Cosmological dynamics of interacting dark energy models in modified gravity", Gravit. Cosmol. **28**, 70 (2022). DOI: 10.1134/S020228932201009X

[30] Y.N. Obukhov and D. Puetzfeld, "Conservation laws in gravity: A unified framework", Phys. Rev. D **104**, 044031 (2021). DOI: 10.1103/PhysRevD.104.044031

[31] Raja Solanki, Avik De, P.K. Sahoo, "Cosmological dynamics of dark energy models in modified gravity", Phys. Dark Universe **36**, 100996 (2022). DOI: 10.1016/j.dark.2022.100996

[32] M. Hohmann, L. Jarv, U. Ualikhanova, "Covariant formulation of scalar-torsion gravity", Phys. Rev. D **96**, 043508 (2017). DOI: 10.1103/PhysRevD.96.043508

[33] A. Samaddar, S. Surendra Singh, "Reconstructing cosmic expansion in $f(R,G)$ gravity using a log-periodic deceleration model", Physics of the Dark Universe, **50**, 102081 (2025). DOI: https://doi.org/10.1016/j.dark.2025.102081

[34] A. Samaddar, S. Surendra Singh, "Exploring the Dynamics of Dark Energy in $f(Q,C)$ Gravity: A Comprehensive Analysis Using Cosmological Datasets", Astron. Lett. **51**, 49 (2025). DOI: https://doi.org/10.1134/S1063773725700203

[35] U. Sarkar, S. Surendra Singh, and A. Samaddar, "Stability analysis of cosmological model in $f(T)$ gravity", Modern Physics Letters A, **40**, 02, 2450206 (2025). DOI: 10.1142/S02177323245020672450206-1

[36] Amit Samaddar and Surendra Sanasam "Dynamical system method of viscous fluid in $f(T)$ gravity theory", Phys. Scr. **99**, 035219 (2024). DOI: 10.1088/1402-4896/ad232a

[37] A. Samaddar, S. Surendra Singh, "Constraining Hořava-Lifshitz gravity with late-time cosmology", Phys. Dark Univ., **49**, 102030 (2025). DOI: 10.1016/j.dark.2025.102030

[38] D. F. Mackey et al., "emcee: The MCMC Hammer", Publ. Astron. Soc. Pac., **125**, 306 (2013). DOI: https://doi.org/10.1086/670067

[39] M. Moresco et al., "Improved constraints on the expansion rate of the Universe up to $z \sim 1.1$ from the spectroscopic evolution of cosmic chronometers", J. Cosmol. Astropart. Phys. **08**, 006 (2012). DOI: https://doi.org/10.1088/1475-7516/2012/08/006

[40] A. Samaddar, S. S. Singh, "Dynamical System Approach and Thermodynamical Perspective of Hořava-Lifshitz Gravity", Fortschritte der Physik, **72**(6), 2400006 (2024). DOI: 10.1002/prop.202400006

[41] A. Samaddar, S. Surendra Singh, "Observational and stability analysis of viscosity-driven cosmic acceleration in $f(Q,C)$ gravity", High Energy Density Physics **56**, 101216 (2025). DOI: 10.1016/j.hedp.2025.101216

[42] DESI Collaboration: M. Abdul-Karim, et al., "DESI DR2 Results II: Measurements of Baryon Acoustic Oscillations and Cosmological Constraints", ArXiv. DOI: https://arxiv.org/abs/2503.14738.

[43] J. P. Hu et al., "Testing the cosmological principle with the Pantheon+ sample and the region-fitting method", A&A, **681**, A88 (2024). DOI: https://doi.org/10.1051/0004-6361/202347121.

[44] A.G. Riess et al., "A Comprehensive Measurement of the Local Value of the Hubble Constant with 1 km/s/Mpc Uncertainty from the Hubble Space Telescope and the SH0ES Team", Astrophys. J. Lett. **934**, (2022) L7. DOI: https://doi.org/10.3847/2041-8213/ac5c5b

[45] R. E. Keeley, A. Shafieloo, and B. L'Huillier, "An Analysis of Variance of the Pantheon+ Dataset: Systematics in the Covariance Matrix?", Universe, **10**, (12), 439 (2024). DOI: https://doi.org/10.3390/universe10120439

[46] Planck Collaboration, Aghanim, N., et al., "Planck 2018 results. VI. Cosmological parameters", Astronomy & Astrophysics, **641**, A6 (2020). DOI: https://doi.org/10.1051/0004-6361/201833910

[47] A. Samaddar, S. Surendra Singh, "Constraining dark energy evolution in $f(Q, C)$ gravity using observational datasets and geometric diagnostics", Journal of High Energy Astrophysics, **48**, 100404 (2025). DOI: 10.1016/j.jheap.2025.100404

[48] A. Samaddar, S. Surendra Singh, "Observational viability of generalized Chaplygin gas in $f(Q, L_m)$ gravity", Astrophys Space Sci **370**, 92 (2025). DOI: 10.1007/s10509-025-04483-y

[49] A. Samaddar, S. Surendra Singh, Md Khurshid Alam, "Dynamical system approach of interacting dark energy models with minimally coupled scalar field", International Journal of Modern Physics D, **32**(09), 2350062 (2023). DOI: 10.1142/S0218271823500621

[50] H. Chaudhary et al "Impact of Interacting Parameters on Dark Matter in an Interacting Dark Energy Model", ApJS **278**, 22 (2025). DOI: 10.3847/1538-4365/adc679

[51] J.D. Bekenstein, "Black Holes and the Second Law", Lett. Nuovo Cim. **4**, 737 (1972). DOI: https://doi.org/10.1007/bf02757029

[52] J.D. Bekenstein, "Black Holes and Entropy", Phys. Rev. D **7**, 2333 (1973). DOI: https://doi.org/10.1103/PhysRevD.7.2333

[53] C. Tsallis, "Possible generalization of Boltzmann-Gibbs statistics", J. Statist. Phys. **52**, 479 (1988). DOI: https://doi.org/10.1007/BF01016429

[54] C. Tsallis, L.J.L. Cirto, "Black hole thermodynamical entropy", Eur. Phys. J. C **73**, 2487 (2013). DOI: https://doi.org/10.1140/epjc/s10052-013-2487-6

[55] F.K. Anagnostopoulos, S. Basilakos, E.N. Saridakis, "Observational constraints on Barrow holographic dark energy", Eur. Phys. J. C **80**, 826 (2020). DOI: https://doi.org/10.1140/epjc/s10052-020-8360-5

[56] A. Sheykhi, "Thermodynamics of interacting holographic dark energy with the apparent horizon as an IR cutoff", Class. Quantum Grav. **27**, 025007 (2010). DOI: https://doi.org/10.1088/0264-9381/27/2/025007

[57] V. Sahni, A. Shafieloo, A.A. Starobinsky, "Two new diagnostics of dark energy", Phys. Rev. D **78**, 103502 (2008). DOI: https://doi.org/10.1103/PhysRevD.78.103502